

# Oxide ionic conductivities of apatite-type lanthanum silicates and germanates and their possibilities as an electrolyte of lower temperature operating SOFC

Yoshikatsu Higuchi<sup>a</sup>, Masayuki Sugawara<sup>a</sup>, Koji Onishi<sup>b</sup>,  
Masatomi Sakamoto<sup>c</sup>, Susumu Nakayama<sup>d,\*</sup>

<sup>a</sup> Honda Research and Development Co., Ltd., Wako-shi 351-0193, Japan

<sup>b</sup> Department of Electrical Engineering and Information Science, Niihama National College of Technology, Niihama-shi 792-8580, Japan

<sup>c</sup> Department of Material and Biological Chemistry, Faculty of Science, Yamagata University, Yamagata-shi 990-8560, Japan

<sup>d</sup> Department of Applied Chemistry and Biotechnology, Niihama National College of Technology, 7-1 Yagumo-cho, Niihama-shi 792-8580, Japan

Received 24 February 2009; received in revised form 1 October 2009; accepted 24 October 2009

Available online 20 November 2009

## Abstract

Electrical properties of  $\text{La}_x\text{M}_6\text{O}_{12+1.5x}$  ( $\text{M} = \text{Si}, \text{Ge}$ ) as an electrolyte for solid oxide fuel cell (SOFC) have been investigated. In  $\text{La}_x\text{Si}_6\text{O}_{12+1.5x}$  and  $\text{La}_x\text{Ge}_6\text{O}_{12+1.5x}$  of  $x = 8\text{--}11$ , the highest conductivities were achieved at  $x = 9.7$  ( $\text{La}_{9.7}\text{Si}_6\text{O}_{26.55}$ ) and  $x = 9.0$  ( $\text{La}_{9.0}(\text{GeO}_4)_6\text{O}_{1.5}$ ), respectively. The conductivity of  $\text{La}_{9.0}(\text{GeO}_4)_6\text{O}_{1.5}$  was higher than that of  $\text{La}_{9.7}\text{Si}_6\text{O}_{26.55}$  in a temperature region higher than 700 °C, and the conductivity ( $2.4 \times 10^{-3} \text{ S cm}^{-1}$ ) of  $\text{La}_{9.7}\text{Si}_6\text{O}_{26.55}$  at 400 °C was higher than that ( $8.3 \times 10^{-5} \text{ S cm}^{-1}$ ) of  $\text{La}_{9.0}(\text{GeO}_4)_6\text{O}_{1.5}$ . The power densities of SOFC ( $\text{H}_2 \mid \text{Pt} \mid \text{electrolyte (thickness: 1 mm)} \mid \text{Pt} \mid \text{O}_2$ ) using  $\text{La}_{9.0}(\text{GeO}_4)_6\text{O}_{1.5}$  as an electrolyte were  $14.3 \text{ mW cm}^{-2}$  (700 °C) and  $24.0 \text{ mW cm}^{-2}$  (800 °C). The corresponding SOFC using  $\text{La}_{9.7}\text{Si}_6\text{O}_{26.55}$  was found to work even at lower temperatures of 400 and 500 °C with power densities of 0.011 and  $0.12 \text{ mW cm}^{-2}$ . The SOFC ( $\text{H}_2 \mid \text{Ni-Sm}_{0.2}\text{Ce}_{0.8}\text{O}_{1.9} \mid \text{electrolyte} \mid \text{Ba}_{0.5}\text{Sr}_{0.5}\text{Co}_{0.8}\text{Fe}_{0.2}\text{O}_{2.5} \mid \text{air}$ ) using 0.3 mm thickness  $\text{La}_{9.7}\text{Si}_6\text{O}_{26.55}$  electrolyte gave the  $3.4 \text{ mW cm}^{-2}$  power density at 500 °C.

© 2009 Elsevier Ltd and Techna Group S.r.l. All rights reserved.

**Keywords:** Electrical properties; Fuel cells

## 1. Introduction

Researches of solid oxide fuel cells (SOFCs) have attracted much attention for the development of environmentally friendly energy-generating systems. In general, yttria stabilized zirconia (YSZ), which shows high ionic conductivity at elevated temperatures, has been used as the most popular electrolyte of these SOFCs. However, some problems, including material selections, cell shielding and lifetime, have been pointed out in the design of such high temperature operating SOFCs. In order to overcome these problems, recent studies have also been directed to the development of the SOFCs operating at lower temperature. The  $\text{LaGaO}_3$ -based perovskite-type oxides reported by Ishihara and his co-workers are the candidates for superior electrolytes which have high ionic conductivity at

relatively lower temperature [1–4]. Rare earth silicates and rare earth germanates with apatite type structure are also another promising candidates. Electrical properties of rare earth silicates has been investigated since 1995 [5–7], and the anisotropy in ionic conductivities have been revealed, using single crystals, that is, the conductivity of a parallel component to  $c$ -axis was higher about one order of magnitude, compared with that of a perpendicular component [8–10]. Of these rare earth silicates, many studies on the ionic conductivities of lanthanum silicates have been reported [11–20]. In particular, magnesium doped lanthanum silicate ( $\text{La}_{9.6}\text{Si}_{5.7}\text{Mg}_{0.3}\text{O}_{26.1}$ ) showed higher conductivity than yttria stabilized zirconia below 780 °C, and the solid oxide fuel cell using  $\text{La}_{9.6}\text{Si}_{5.7}\text{Mg}_{0.3}\text{O}_{26.1}$  as an electrolyte was found to work around 700 °C with power density  $35 \text{ mW cm}^{-2}$  [20]. For these apatite-type ionic conductors, some oxide ion conduction mechanisms have been proposed [13,16,19]. On the other hand, lanthanum germanates,  $\text{La}_x\text{Ge}_6\text{O}_{12+1.5x}$ , in which  $\text{SiO}_4$  unit is

\* Corresponding author. Tel.: +81 897 37 7786; fax: +81 897 37 7777.

substituted with  $\text{GeO}_4$  unit, was also found to show high ionic conductivity [21,22]. In this work, the relationship between the La amount in apatite type  $\text{La}_x\text{M}_6\text{O}_{12+1.5x}$  ( $\text{M} = \text{Si}, \text{Ge}$ ) ceramics and their ionic conductivities was examined, and the SOFC characteristics were investigated using these electrolyte materials in the range of 400–800 °C.

## 2. Experimental procedure

In preparation of  $\text{La}_x\text{M}_6\text{O}_{12+1.5x}$  ( $\text{M} = \text{Si}, \text{Ge}$ ),  $\text{La}_2\text{O}_3$  and  $\text{SiO}_2$  or  $\text{GeO}_2$  were mixed under the desired ratios in the plastic pot in which zirconia balls were placed. Each mixture was ball-milled for 20 h, dried and calcined in alumina crucible for 2 h. Calcination temperatures were at 1200 and 1000 °C for silicate and germanate, respectively. The resulting powders were again ball-milled into fine powders for 20 h. Then, discs were prepared by pressing the powders under 100 MPa, and sintered for 2 h at 1700 and 1500 °C for silicate and germanate, respectively. The discs were 10 mm diameter and 1 mm thickness after sintering. After both sides of the disc were coated with Pt paste, the disc was baked at 1000 °C.

Crystal parameters were determined by the measurement of powder X-ray diffraction (XRD, Rigaku MiniFlex) using  $\text{CuK}\alpha$  radiation in the  $2\theta$  range of 10–70°. Electrical properties were measured in the temperature range of 400–800 °C and in the frequency range of 100 Hz to 10 MHz with an impedance analyzer HP4194A. Conductivities were determined applying the complex plane impedance analysis. The complex impedance plot in the lower temperatures was represented by a semicircle, probably corresponding to the bulk component, which passed through the origin in the high frequency region and had a spike, probably arising from the electrolyte–electrode behavior, in the low frequency region. The semicircle attributable to the grain boundary component was not observed, probably because the resistance of its component is fairly lower compared with that of bulk component. When the temperature was increased, the semicircle was diminished and only a spike was observed. SOFC characteristics were evaluated using a test cell, in which both faces of the sample disk (thickness: 1 mm) were glass-sealed into alumina tubes and attached to Pt meshes with Pt leads. Open circuit voltage (OCV) was measured and evaluation of the  $I$ – $V$  curve were made at 400 and 500 °C for silicate and at 700 and 800 °C for germanate, with  $\text{H}_2$  being introduced at a rate of  $10 \text{ cm}^3 \text{ min}^{-1}$  to the anode and  $\text{O}_2$  to the cathode at a rate of  $20 \text{ cm}^3 \text{ min}^{-1}$ . Single cell performance of the SOFC using lanthanum silicate (thickness: 0.3 and 1 mm) as an electrolyte,  $\text{Ba}_{0.5}\text{Sr}_{0.5}\text{Co}_{0.8}\text{Fe}_{0.2}\text{O}_{2.5}$  (BSCF) as an anode and  $\text{Ni-Sm}_{0.2}\text{Ce}_{0.8}\text{O}_{1.9}$  (SDC) as a cathode was evaluated at 500 °C with  $\text{H}_2$  being introduced at a rate of  $15 \text{ cm}^3 \text{ min}^{-1}$  to the anode and air to the cathode at a rate of  $20 \text{ cm}^3 \text{ min}^{-1}$ . Here, BSCF and Ni–SDC powders were synthesized by the usual oxide mixing method and were dispersed in terpeneol. After one side of the electrolyte disk was coated using the dispersed BSCF powders and another side was coated using the dispersed Ni–SDC powders, these were heated to 1300 °C for 1 h.

## 3. Results and discussion

Fig. 1(a) shows the conductivities of  $\text{La}_x\text{Si}_6\text{O}_{12+1.5x}$  ( $x = 8.0, 9.0, 9.33, 9.4, 9.5, 9.6, 9.7, 9.8, 10.0$  and  $11.0$ ) at 400, 500, 600, 700 and 800 °C. At each temperature, an abrupt increase of conductivity was observed around  $x = 9.4$  or  $9.5$ , as  $x$  was changed from 8.0 to 11.0, and conductivities were higher in the region of  $x = 9.6$ –11.0 than those in the region of  $x = 8.0$ –9.33. The highest conductivity was achieved at  $x = 9.7$ . The XRD results suggested that  $\text{La}_x\text{Si}_6\text{O}_{12+1.5x}$  ceramics were the apatite single phase in the range of  $x = 8$ –9.33. In the range of  $x = 9.4$ –11,  $\text{La}_2\text{SiO}_5$  as a minor phase was found to form in addition to the main apatite ( $\text{La}_x(\text{SiO}_4)_6\text{O}_{1.5x-12}$ ) phase. The lattice constants of the main apatite phase ( $a = 0.973 \text{ nm}$ ,  $c = 0.720 \text{ nm}$ ) were little changed by an increase in  $x$  value.

Conductivities of  $\text{La}_x\text{Ge}_6\text{O}_{12+1.5x}$  ( $x = 8.0, 9.0, 9.1, 9.2, 9.33, 10.0$  and  $11.0$ ) at 500, 600, 700 and 800 °C were shown in Fig. 1(b). Contrary to the  $\text{La}_x\text{Si}_6\text{O}_{12+1.5x}$ , conductivities were higher in the region of  $x = 8$ –9.33 than those in the region of  $x = 10.0$ –11.0. The highest conductivity was achieved at  $x = 9.0$ , where the number of  $\text{La}^{3+}$  at the  $4f + 6h$  sites is 9.0 and the number of oxide ion at the  $2a$  site is 1.5. As was also the case for

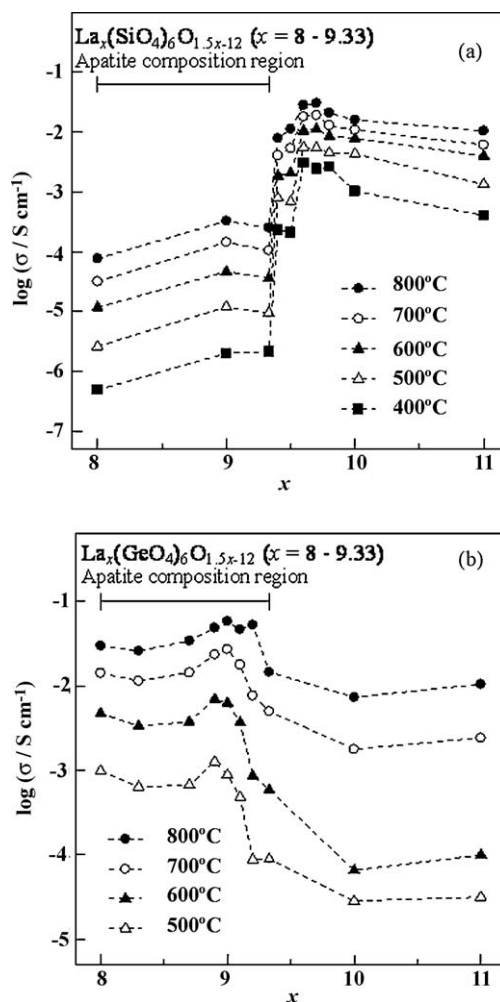


Fig. 1. Relationship between the conductivities and  $x$  values of (a)  $\text{La}_x\text{Si}_6\text{O}_{12+1.5x}$  and (b)  $\text{La}_x\text{Ge}_6\text{O}_{12+1.5x}$ .

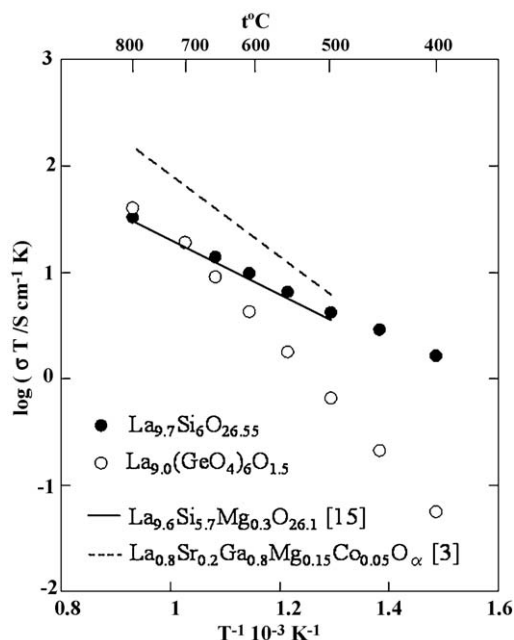


Fig. 2. Temperature dependence of the conductivity.

$\text{La}_x\text{Si}_6\text{O}_{12+1.5x}$ . XRD results revealed that the apatite single phase was formed in  $x = 8.0$ – $9.33$ , whereas  $\text{La}_2\text{GeO}_5$  phase was formed in  $x = 10.0$  and  $11.0$  in addition to the main apatite ( $\text{La}_x(\text{GeO}_4)_6\text{O}_{1.5x-12}$ ) phase. The lattice constants of the main apatite phase ( $a = 0.991$  nm,  $c = 0.727$  nm), which are larger than those of  $\text{La}_x(\text{SiO}_4)_6\text{O}_{1.5x-12}$ , were also little changed by an increase in  $x$  value in the range of  $x = 8$ – $11$ . Evaporation of  $\text{GeO}_2$  from  $\text{La}_{9.0}(\text{GeO}_4)_6\text{O}_{1.5}$  was examined by measuring the weight loss after sintering at  $1500^\circ\text{C}$ . It was only  $0.15$  wt%, indicating that evaporation of  $\text{GeO}_2$  is almost negligible.

Fig. 2 shows Arrhenius plots of the conductivities for  $\text{La}_{9.7}\text{Si}_6\text{O}_{26.55}$  and  $\text{La}_{9.0}(\text{GeO}_4)_6\text{O}_{1.5}$  which gave the highest ionic conductivity in a series of  $\text{La}_x\text{M}_6\text{O}_{12+1.5x}$  ( $\text{M} = \text{Si}, \text{Ge}$ ),

together with that for the  $\text{La}_{9.6}\text{Si}_{5.7}\text{Mg}_{0.3}\text{O}_{26.1}$  [15]. In the temperature range of  $500$ – $800^\circ\text{C}$ , the ionic conductivity of  $\text{La}_{9.7}\text{Si}_6\text{O}_{26.55}$  was slightly higher than that of  $\text{La}_{9.6}\text{Si}_{5.7}\text{Mg}_{0.3}\text{O}_{26.1}$ . The former lanthanum silicate is expected to show slightly higher conductivity than the latter Mg doped lanthanum silicate also below  $500^\circ\text{C}$ , though the conductivities of the Mg doped lanthanum silicates are not reported. Temperature dependence of ionic conductivities of  $\text{La}_{9.0}(\text{GeO}_4)_6\text{O}_{1.5}$  was much remarkable, compared with  $\text{La}_{9.7}\text{Si}_6\text{O}_{26.55}$  and  $\text{La}_{9.6}\text{Si}_{5.7}\text{Mg}_{0.3}\text{O}_{26.1}$ . Above  $700^\circ\text{C}$ ,  $\text{La}_{9.0}(\text{GeO}_4)_6\text{O}_{1.5}$  exhibited slightly higher conductivity than  $\text{La}_{9.7}\text{Si}_6\text{O}_{26.55}$ . Below  $650^\circ\text{C}$ , conductivities of  $\text{La}_{9.0}(\text{GeO}_4)_6\text{O}_{1.5}$  were the lowest, and conductivity at  $400^\circ\text{C}$  was  $8.3 \times 10^{-5} \text{ S cm}^{-1}$  which is  $1.5 \times 10^1$  times lower than that ( $2.4 \times 10^{-3} \text{ S cm}^{-1}$ ) of  $\text{La}_{9.7}\text{Si}_6\text{O}_{26.55}$ . Conductivities of the present lanthanum silicate ( $\text{La}_{9.7}\text{Si}_6\text{O}_{26.55}$ ) were lower than those of lanthanum gallate ( $\text{La}_{0.8}\text{Sr}_{0.2}\text{Ga}_{0.8}\text{Mg}_{0.15}\text{Co}_{0.05}\text{O}_\alpha$ ) reported in the literature [3].

Figs. 3 and 4 show the impedance plots of  $\text{La}_{9.7}\text{Si}_6\text{O}_{26.55}$  at  $200$ ,  $300$ ,  $400$  and  $500^\circ\text{C}$  and  $\text{La}_{9.0}(\text{GeO}_4)_6\text{O}_{1.5}$  at  $400$ ,  $500$ ,  $700$  and  $800^\circ\text{C}$ , respectively. In the lower temperatures, the result was represented by a semicircle, probably corresponding to the bulk component, which passed through the origin in the high frequency region and had a spike, probably arising from the electrolyte–electrode behavior, in the low frequency region [7,15]. The semicircle attributable to the grain boundary component was not observed, probably because the resistance of grain boundary is fairly low, compared with that of bulk component. When the temperature was increased, the semicircle diminished and only a spike was observed. At  $500^\circ\text{C}$  of  $\text{La}_{9.7}\text{Si}_6\text{O}_{26.55}$  and  $700$  and  $800^\circ\text{C}$  of  $\text{La}_{9.0}(\text{GeO}_4)_6\text{O}_{1.5}$ , the spikes were observed as the semicircles. From these results, the resistances of the bulk were shown by an arrow in Figs. 3 and 4.

Characteristics of the solid oxide fuel cells, ( $\text{H}_2 | \text{Pt} | \text{electrolyte} | \text{Pt} | \text{O}_2$ ) were investigated, where

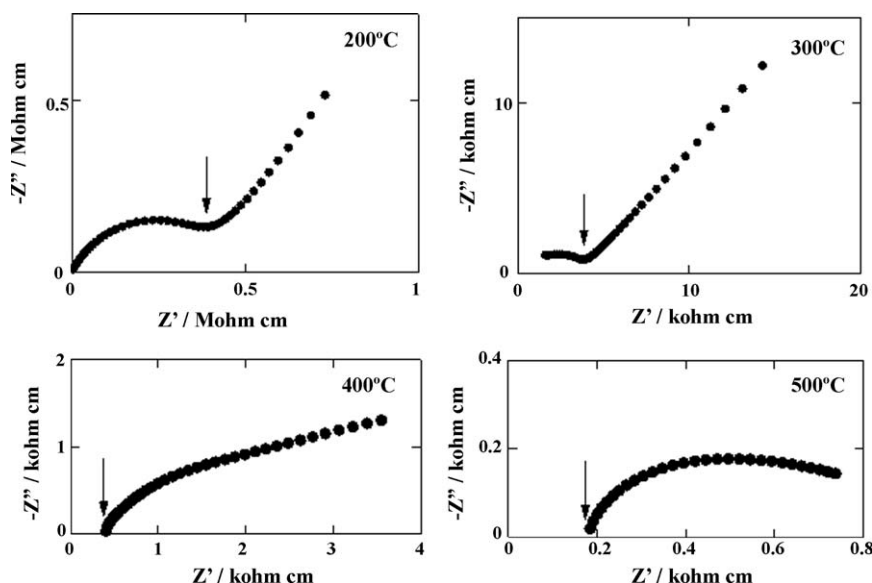


Fig. 3. Complex impedance plots of  $\text{La}_{9.7}\text{Si}_6\text{O}_{26.55}$  at  $200$ ,  $300$ ,  $400$  and  $500^\circ\text{C}$ .

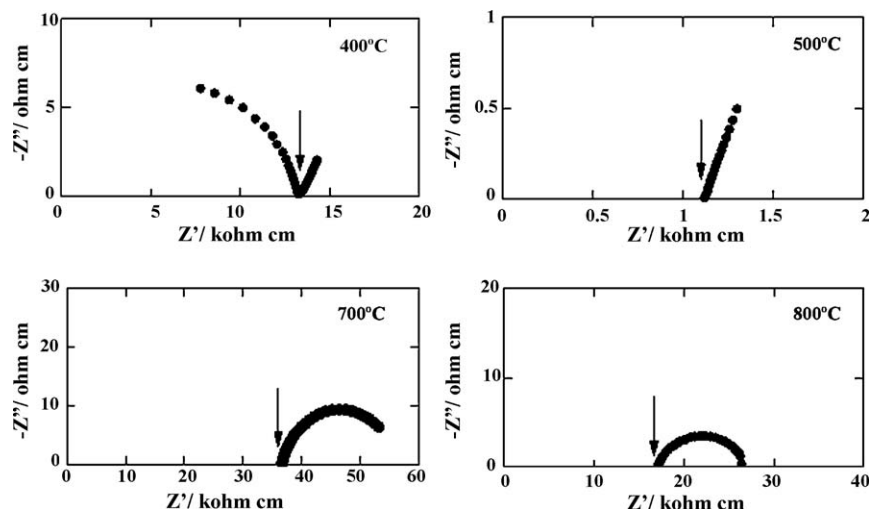


Fig. 4. Complex impedance plots of  $\text{La}_{9.0}(\text{GeO}_4)_6\text{O}_{1.5}$  at 400, 500, 700 and 800 °C.

$\text{La}_{9.0}(\text{GeO}_4)_6\text{O}_{1.5}$  or  $\text{La}_{9.7}\text{Si}_6\text{O}_{26.55}$  was used as an electrolyte (Fig. 5). The SOFC with apatite type ionic conductors, was reported for the cell ( $\text{H}_2 \mid \text{Pt} \mid \text{La}_{9.6}\text{Si}_{5.7}\text{Mg}_{0.3}\text{O}_{26.1} \mid \text{Pt} \mid \text{N}_2\text{--O}_2$  (20%)) using  $\text{La}_{9.6}\text{Si}_{5.7}\text{Mg}_{0.3}\text{O}_{26.1}$  electrolyte (1 mm thickness) [15]. Its maximum power densities were  $20.0 \text{ mW cm}^{-2}$  at 805 °C,  $5.8 \text{ mW cm}^{-2}$  at 706 °C, and  $1.3 \text{ mW cm}^{-2}$  at 608 °C, suggesting that  $\text{La}_{9.6}\text{Si}_{5.7}\text{Mg}_{0.3}\text{O}_{26.1}$  can operate around 600 °C as a solid electrolyte of SOFC. When  $\text{La}_{9.0}(\text{GeO}_4)_6\text{O}_{1.5}$  electrolyte was used in the cell, the maximum power densities achieved were 23.0 and  $14.1 \text{ mW cm}^{-2}$  at 800 and 700 °C,

respectively (Fig. 5(a)). At these temperatures, conductivities of  $\text{La}_{9.0}(\text{GeO}_4)_6\text{O}_{1.5}$  were higher than those of  $\text{La}_{9.7}\text{Si}_6\text{O}_{26.55}$  and  $\text{La}_{9.6}\text{Si}_{5.7}\text{Mg}_{0.3}\text{O}_{26.1}$ , as described above (see Fig. 2). These maximum values are comparable to, or slightly higher than those reported by Yoshioka and Tanase. Below 650 °C, conductivities of  $\text{La}_{9.7}\text{Si}_6\text{O}_{26.55}$  were higher than those of  $\text{La}_{9.0}(\text{GeO}_4)_6\text{O}_{1.5}$  and  $\text{La}_{9.6}\text{Si}_{5.7}\text{Mg}_{0.3}\text{O}_{26.1}$  (also see Fig. 2). In the lower temperature range, maximum power densities of the cell with  $\text{La}_{9.7}\text{Si}_6\text{O}_{26.55}$  electrolyte were determined:  $0.12 \text{ mW cm}^{-2}$  at 500 °C and  $0.011 \text{ mW cm}^{-2}$  at 400 °C (Fig. 5(b)). These maximum power densities achieved at 800 and 700 °C for the cell designed from  $\text{La}_{9.0}(\text{GeO}_4)_6\text{O}_{1.5}$  electrolyte and at 500 and 400 °C for the cell designed from  $\text{La}_{9.7}\text{Si}_6\text{O}_{26.55}$  electrolyte were significantly lower than those theoretically estimated by considering only an electrical resistance of electrolyte. However, the present work demonstrated that the  $\text{La}_{9.7}\text{Si}_6\text{O}_{26.55}$  electrolyte can operate as SOFC even at the lower temperature around 400 °C.

The use of Ni–SDC anode and BSCF cathode was tried, in order to improve the power density. It was recently reported that a cell using  $\text{La}_{9.8}\text{Si}_{5.7}\text{Mg}_{0.3}\text{O}_{26.4}$  (thickness: 1 mm), Ni–SDC and  $\text{La}_{0.9}\text{Sr}_{0.1}\text{CoO}_{3-\delta}$  as an electrolyte, an anode and a cathode, respectively, shows maximum power densities of  $120 \text{ mW cm}^{-2}$  at 800 °C and  $35 \text{ mW cm}^{-2}$  at 700 °C [20]. Fig. 6 shows performance curves measured at 500 °C of the SOFC prepared using 1 and 0.3 mm thick  $\text{La}_{9.7}\text{Si}_6\text{O}_{26.55}$  disk as an electrolyte. Power density reached the maximum values of 1.2 and  $3.4 \text{ mW cm}^{-2}$  for 1 mm thick and 0.3 mm thick, respectively, indicating that electrode materials contribute to the improvement. Assuming that the ratio of the electrolyte resistance to the whole cell resistance is much large, power density of the cell is significantly influenced by the resistance of the electrolyte [4]. Indeed, power density of the electrolyte of the thickness 0.3 mm was about three times that of the electrolyte of the thickness 1 mm. Similarly, power density of LSGMC, which was  $120 \text{ mW cm}^{-2}$  for 40  $\mu\text{m}$  thickness [4], can be estimated to be  $16 \text{ mW cm}^{-2}$  for 0.3 mm thickness. This value is higher than  $3.4 \text{ mW cm}^{-2}$  of the present  $\text{La}_{9.7}\text{Si}_6\text{O}_{26.55}$  (0.3 mm thickness), suggesting that the difference between the

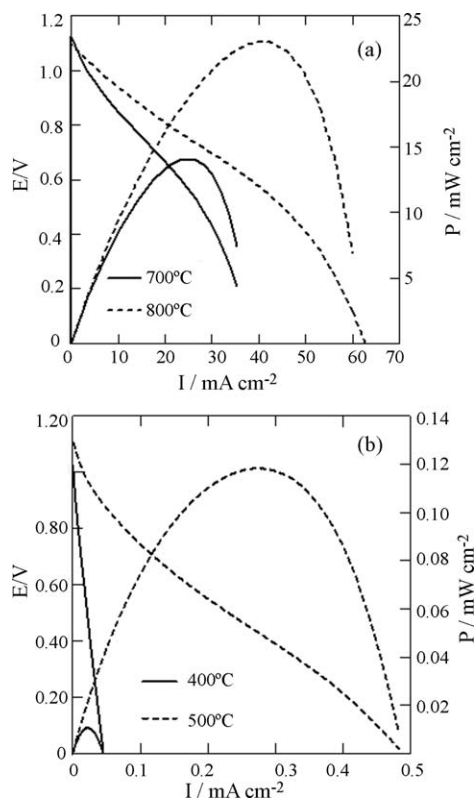


Fig. 5.  $I$ – $V$  curves and power densities of the solid oxide fuel cells ( $\text{H}_2 \mid \text{Pt} \mid$  electrolyte (thickness: 1 mm)  $\mid \text{Pt} \mid \text{O}_2$ ) using (a)  $\text{La}_{9.0}(\text{GeO}_4)_6\text{O}_{1.5}$  and (b)  $\text{La}_{9.7}\text{Si}_6\text{O}_{26.55}$  as electrolyte.

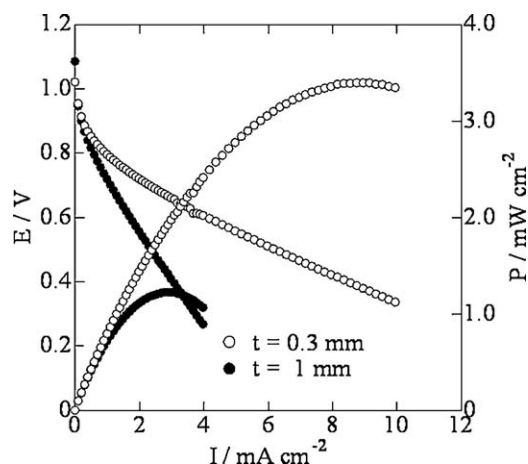


Fig. 6.  $I$ - $V$  curves and power densities at 500 °C of the solid oxide fuel cells ( $\text{H}_2$  |  $\text{Ni-Sm}_{0.2}\text{Ce}_{0.8}\text{O}_{1.9}$  | electrolyte (thickness: 0.3 and 1 mm) |  $\text{Ba}_{0.5}\text{Sr}_{0.5}\text{Co}_{0.8}\text{Fe}_{0.2}\text{O}_{2.5}$  | air) using  $\text{La}_{0.7}\text{Si}_6\text{O}_{26.55}$  as electrolyte.

conductivities of these two electrolytes give a significant effect on the power density. Further researches/improvements on the electrolyte materials and cell structure are in progress for the development of SOFC using apatite-type lanthanum silicate and germanate ceramics.

#### 4. Conclusions

In a series of apatite-type  $\text{La}_x\text{M}_6\text{O}_{12+1.5x}$  ( $\text{M} = \text{Si, Ge}$ ,  $x = 8$ –11) ceramics,  $\text{La}_{9.7}\text{Si}_6\text{O}_{26.55}$  and  $\text{La}_{9.0}(\text{GeO}_4)_6\text{O}_{1.5}$  were found to show the higher conductivities.

$\text{La}_{9.0}(\text{GeO}_4)_6\text{O}_{1.5}$  exhibited higher conductivity than  $\text{La}_{9.7}\text{Si}_6\text{O}_{26.55}$  above 700 °C, and vice versa below 650 °C. Conductivities of  $\text{La}_{9.0}(\text{GeO}_4)_6\text{O}_{1.5}$  and  $\text{La}_{9.7}\text{Si}_6\text{O}_{26.55}$  were  $2.7 \times 10^{-2} \text{ S cm}^{-1}$  (700 °C) and  $2.4 \times 10^{-3} \text{ S cm}^{-1}$  (400 °C), respectively.

Power densities of SOFCs ( $\text{H}_2$  | Pt | electrolyte (thickness: 1 mm) | Pt |  $\text{O}_2$ ) using  $\text{La}_{9.0}(\text{GeO}_4)_6\text{O}_{1.5}$  and  $\text{La}_{9.7}\text{Si}_6\text{O}_{26.55}$  as an electrolyte were  $14.3 \text{ mW cm}^{-2}$  (700 °C) and  $0.011 \text{ mW cm}^{-2}$  (400 °C), respectively.

The power density on the SOFC ( $\text{H}_2$  | Ni-SDC |  $\text{La}_{9.7}\text{Si}_6\text{O}_{26.55}$  (thickness: 0.3 mm) | BSCF | air) was  $3.4 \text{ mW cm}^{-2}$  at 500 °C, where Ni-SDC and BSCF were used as anode and cathode materials, respectively, instead of Pt.

#### References

- [1] T. Ishihara, H. Matsuda, Y. Takita, Doped  $\text{LaGaO}_3$  perovskite type oxide as a new oxide ionic conductor, *J. Am. Chem. Soc.* 116 (1994) 3801–3803.
- [2] T. Ishihara, H. Matsuda, Y. Takita, Effects of rare earth cations doped for La site on the oxide ionic conductivity of  $\text{LaGaO}_3$ -based perovskite type oxide, *Solid State Ionics* 79 (1995) 147–151.

- [3] K. Kuroda, I. Hashimoto, K. Adachia, J. Akikusa, Y. Tamou, N. Komada, T. Ishihara, Y. Takita, Characterization of solid oxide fuel cell using doped lanthanum gallate, *Solid State Ionics* 132 (2000) 199–208.
- [4] T. Ishihara, J. Tabuchi, S. Ishikawa, J. Yan, M. Enoki, H. Matsumoto, Recent progress in  $\text{LaGaO}_3$  based solid electrolyte for intermediate temperature SOFCs, *Solid State Ionics* 177 (2006) 1949–1953.
- [5] S. Nakayama, H. Aono, Y. Sadaoka, Ionic conductivity of  $\text{Ln}_{10}(\text{SiO}_4)_6\text{O}_3$  ( $\text{Ln} = \text{La, Nd, Sm, Gd}$  and  $\text{Dy}$ ), *Chem. Lett.* 24 (1995) 431–432.
- [6] S. Nakayama, T. Kageyama, H. Aono, Y. Sadaoka, Ionic conductivity of lanthanoid silicates,  $\text{Ln}_{10}(\text{SiO}_4)_6\text{O}_3$  ( $\text{Ln} = \text{La, Nd, Sm, Gd, Dy, Y, Ho, Er}$  and  $\text{Yb}$ ), *J. Mater. Chem.* 5 (1995) 1801–1805.
- [7] S. Nakayama, M. Sakamoto, Electrical properties of new type high oxide ionic conductor  $\text{RE}_{10}\text{Si}_6\text{O}_{27}$  ( $\text{RE} = \text{La, Pr, Nd, Sm, Gd, Dy}$ ), *J. Euro. Ceram. Soc.* 18 (1998) 1413–1418.
- [8] S. Nakayama, M. Sakamoto, M. Higuchi, K. Kodaira, M. Sato, S. Kakita, T. Suzuki, K. Itoh, Oxide ionic conductivity of apatite type  $\text{Nd}_{9.33}(\text{SiO}_4)_6\text{O}_2$  single crystal, *J. Euro. Ceram. Soc.* 19 (1999) 507–510.
- [9] M. Higuchi, K. Kodaira, S. Nakayama, Growth of apatite-type neodymium silicate single crystals by the floating-zone method, *J. Cryst. Growth* 207 (1999) 298–302.
- [10] S. Nakayama, M. Higuchi, Electrical properties of apatite type oxide ionic conductors  $\text{RE}_{9.33}(\text{SiO}_4)_6\text{O}_2$  ( $\text{RE} = \text{Pr, Nd}$  and  $\text{Sm}$ ) single crystals, *J. Mater. Sci. Lett.* 20 (2001) 913–915.
- [11] J.E.H. Sansom, D. Richings, P.R. Slater, A powder neutron diffraction study of the oxide-ion-conducting apatite-type phases,  $\text{La}_{9.33}\text{Si}_6\text{O}_{26}$  and  $\text{La}_8\text{Sr}_2\text{Si}_6\text{O}_{26}$ , *Solid State Ionics* 139 (2001) 205–210.
- [12] E.J. Abram, D.C. Sinclair, A.R. West, A novel enhancement of ionic conductivity in the cation-deficient apatite  $\text{La}_{9.33}(\text{SiO}_4)_6\text{O}_2$ , *J. Mater. Chem.* 11 (2001) 1978–1979.
- [13] J.R. Tolchard, M.S. Islam, P.R. Slater, Defect chemistry and oxygen ion migration in the apatite-type materials  $\text{La}_{9.33}(\text{SiO}_4)_6\text{O}_2$  and  $\text{La}_8\text{Sr}_2\text{Si}_6\text{O}_{26}$ , *J. Mater. Chem.* 16 (2003) 1956–1961.
- [14] M. Higuchi, Y. Masubuchi, S. Nakayama, S. Kikkawa, K. Kodaira, Single crystal growth and oxide ion conductivity of apatite-type rare-earth silicates, *Solid State Ionics* 174 (2004) 73–80.
- [15] H. Yoshioka, S. Tanase, Magnesium doped lanthanum silicate with apatite-type structure as an electrolyte for intermediate temperature solid oxide fuel cells, *Solid State Ionics* 176 (2005) 2395–2398.
- [16] Y. Masubuchi, H. Higuchi, T. Takeda, S. Kikkawa, Oxide ion conduction mechanism in  $\text{RE}_{9.33}(\text{SiO}_4)_6\text{O}_2$  and  $\text{Sr}_2\text{RE}_8(\text{SiO}_4)_6\text{O}_2$  ( $\text{RE} = \text{La, Nd}$ ) from neutron powder diffraction, *Solid State Ionics* 177 (2006) 263–268.
- [17] T. Iwata, E. Bechade, K. Fukuoaka, O. Masson, I. Julien, E. Champion, P. Thomas, Lanthanum- and oxygen-deficient structures of oxide-ion conducting apatite-type silicates, *J. Am. Ceram. Soc.* 91 (2008) 3714–3720.
- [18] P.J. Panteix, I. Julien, P. Abelard, D. Bernache-Assollant, Influence of porosity on the electrical properties of  $\text{La}_{9.33}(\text{SiO}_4)_6\text{O}_2$  oxyapatite, *Ceram. Inter.* 34 (2008) 1579–1586.
- [19] R. Ali, M. Yashima, Y. Matsushita, H. Yoshioka, K. Ohoyama, F. Izumi, Diffusion path of oxide ions in an apatite-type ionic conductor  $\text{La}_{9.69}(\text{Si}_{5.70}\text{Mg}_{0.30})\text{O}_{26.24}$ , *Chem. Mater.* 20 (2008) 5203–5208.
- [20] H. Yoshioka, Y. Nojiri, S. Tanase, Ionic conductivity and fuel cell properties of apatite-type lanthanum silicates doped with Mg and containing excess oxide ions, *Solid State Ionics* 179 (2008) 2165–2169.
- [21] H. Arikawa, H. Nishiguchi, T. Ishihara, Y. Takita, Oxide ion conductivity in Sr-doped  $\text{La}_{10}\text{Ge}_6\text{O}_{27}$  apatite oxide, *Solid State Ionics* 136–137 (2000) 31–37.
- [22] S. Nakayama, M. Sakamoto, Ionic conductivities of apatite-type  $\text{La}_x(\text{GeO}_4)_6\text{O}_{1.5x-12}$  ( $x = 8$ –9.33) polycrystals, *J. Mater. Sci. Lett.* 20 (2002) 1627–1629.